EVOLUTION OF GRAPHITIC STRUCTURES IN AMORPHOUS CARBON THIN FILMS

Eiji Iwamura
PRESTO, Japan Science and Technology Agency
CCR, The University of Tokyo, 4-6-1 Komaba, Meguro-ku, Tokyo 153-8904, Japan

e-mail:iwamura@odin.hpm.rcast.u-tokyo.ac.jp

Introduction

Carbon-based materials have been regarded as one of the most important materials in nanotechnology. Not only nanotubes and fullerenes but also a new form of carbon incorporating different graphitic configurations in amorphous carbon networks has recently attracted extensive interests in order to accomplish high performances by combining diverse physical properties which arise from carbon structures. In particular, the establishment of functionally hybridized carbon systems with a thin film form fabricated in a feasible process for practical production would encourage application of these materials in various fields of nanotechnology. Although various techniques for synthesizing graphitic structures together with amorphous carbon have been reported [1-8], the way to control the ordered/disordered carbon structures has not been established yet. In addition, structural ordering of carbon atoms strongly depends on the synthesis processes or requires specific conditions, such as a high-energy electron beam irradiation or a relatively high temperature.

In this study, a new approach to form nanocomposite structures containing graphitic clusters in an amorphous carbon matrix was investigated. A low-energy electron beam radiation system was introduced to modify amorphous carbon networks. Evolution of onion-like structures and nano-crystalline graphitic structures in an amorphous carbon matrix was discussed.

Experimental

Amorphous carbon thin films with 100 nm thickness were deposited onto Si(100) substrates by a sputtering technique. About 15at% of Fe, Co or Ni atoms were doped to the amorphous carbon films by co-sputtering. Subsequently, the pre-formed Me:a-C films were exposed to an electron shower. Figure 1 shows the schmatic diagram of the low-energy electron beam (EB) radiation system. The electrons were accelerated with 60 kV, transmitted through a 3-micron-thick Si window and irradiated to the films placed on a specimen stage. As electrons passed through the window, energy was reduced and the electron beam was scattered. The electron dose showed linear relation to the accelerating voltage and the gap between the Si window and the specimen, and dose rate was 5.8×10^{13} sec^{-1}·cm^{-2} in the condition used in this study. The operating chamber pressure was about 1.3×10^{-3} Pa and remained constant during the irradiation process. As the electron beam emitted, temperature increased up to 450 K at 50 µm underneath

the film surface and 310 K at the specimen stage. Plan-view and cross-sectional microstructures were characterized by a transmission electron microscopy operating at 200 kV. TEM specimens were prepared by back thinning method using $2HF+8HNO_3$ mixture. For plan-view observation, the top surface of the films was etched up to 20-30 nm in thickness by 3%HNO3+metanol mixture.
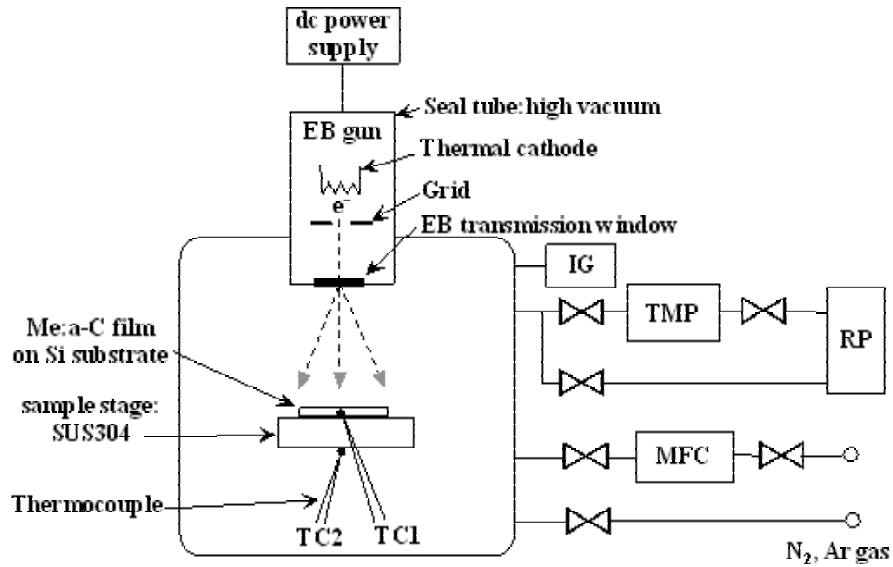

Figure 1. Schematic diagram of low-energy electron radiation system.

Results and Discussion

Figures 2(a)-(C) show cross-sectional TEM micrographs of Fe:a-C films after EB irradiation. At the initial stage of EB irradiation, Fe atoms appeared to be uniformly dispersed in the film. As the irradiation time increased, Fe grains were precipitated. It was observed that iron atoms preferred to diffuse toward to the film surface concurrently with growth of the precipitates. As a result, a large region where Fe became absent was formed in the interior of the film.

Figures 3(a)-(d) show plan-view TEM micrographs of Fe:a-C films before and after EB irradiation. As the surface layer where Fe atoms are segregated is removed, these micrographs show the microstructures of interior of the films. Fig. 3(a) is the as-deposited film showing Fe-rich amorphous clusters with about 1 nm in size uniformly dispersed in the a-C matrix. Fig. 3(b) is the microstructure after EB irradiation for 1.8 ksec. As EB irradiation started, the Fe clusters started to coalesce and crystallization of Fe was occurred. As the grains were isolated to one the others in the a-C matrix, the grain growth was supposed to proceed in the manner of Ostwald ripening. Electron beam diffraction and Mössbauer spectra analyses revealed that the fine Fe grains had face-centered-cubic structure and there were two kinds of fcc-Fe structures which had different contents of interstitial carbon. On this early stage of EB irradiation, graphitization was invisible. Fig. 3(c) is the microstructure after EB irradiation for 9.9 ksec. Growth of the fcc-Fe grains progressed and curved multi-shell structures with the

spacing of graphite c-plane were frequently observed in the a-C matrices. The size of the shell structures and a number of stacks of graphitic layers were increased as the irradiation time increased. With further EB irradiation as shown in Fig. 3(d), a different type of graphitic structures was observed in addition to fragments of the curved multi-shell structures. The graphitic structure appeared not to be distorted but to be a plate-like. The size was about 20-40 nm in length and 10-20 nm in width.
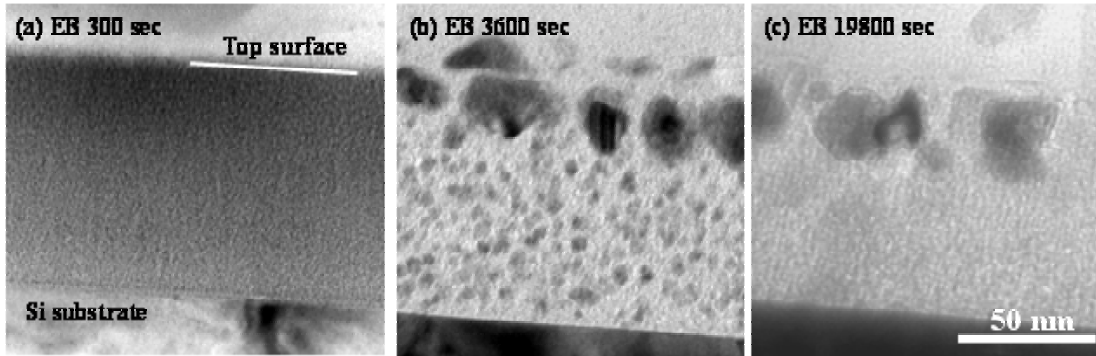

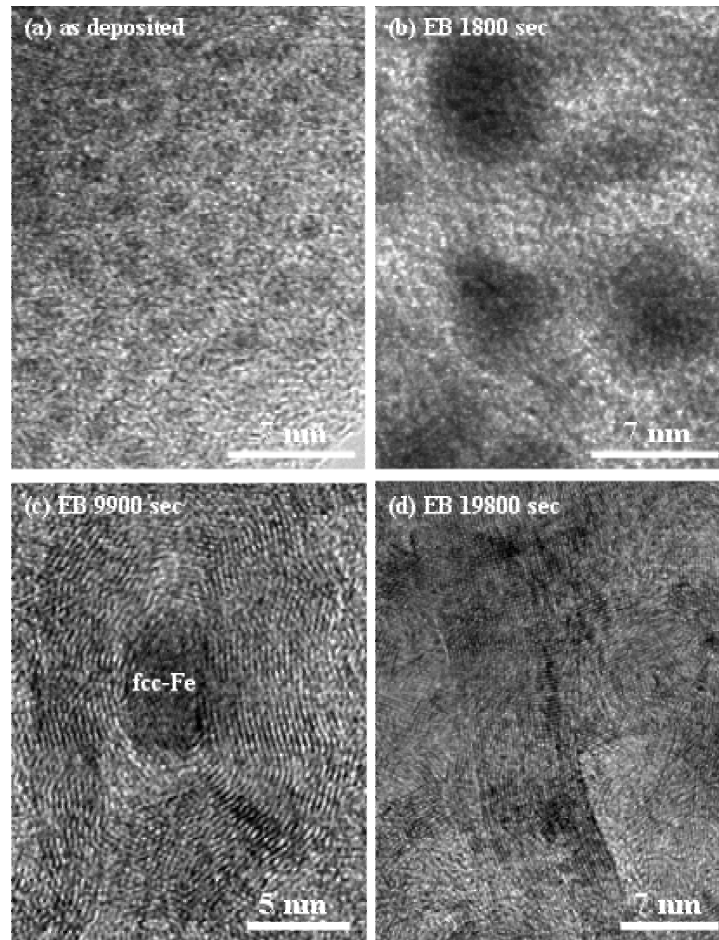Figure 2. Cross-sectional microstructures of Fe:a-C films.

Figure 3. Plan-view microstructures of Fe:a-C films.

Figures 4(a)-(b) show plan-view TEM micrographs with low-magnification of Fe:a-C films after EB irradiation for 9.9 ksec and 19.8 ksec, respectively. As show in Fig. 4(a) with arrows, the curved multi-shell structures were formed dispersedly and the surrounding area appeared to remain amorphous with lower density. On the other hand, the plate-like graphitic clusters exhibited completely different morphology as denoted by a circle in Fig. 4(b). They appeared to form in the region where Fe atoms became absent.
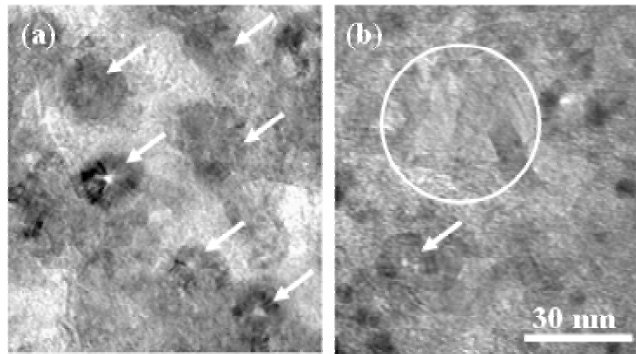

Figure 4. Plan-view micrographs of Fe:a-C films with graphitic inclusions.

The fundamentally same microstructural evolution during EB irradiation was observed in the case of Co:a-C [9] and Ni:a-C as well. However, graphitization behavior in Ni:a-C was slightly different from the others. Figures 5(a)-(c) show plan-view TEM micrographs of a Fe:a-C, Co:a-C and Ni:a-C film, respectively. In the case of the Fe and Co containing films, onion-like structures with relatively small size were observed and most of them had no metal core. On the other hand, graphitization was observed only on the relatively large grains formed in the vicinity of the surface of the Ni:a-C films. The Ni grain size was approximately more than 20 nm, and the Ni grains were encapsulated by onion-like structures.

Figure 6(a) shows the change of average Fe and Ni grain size as a function of EB irradiation time. The size increased following the 1/2 and the 1/3 power law for Fe and Ni, respectively. Figures 6(b)-(c) show size distribution of Fe and Ni grains observed in the interior of the films, respectively. The dotted lines inserted in Fig. 6(b) and (c) are theoretical curves of interface reaction and diffusion controlled growth mechanism, respectively. The observed size distributions clearly show the features of each growth mechanism. The irradiation time dependence of cluster size and its size distribution indicates that the grain growth proceeds in the manner of Ostwald ripening. Interface reaction controls the grain growth in Fe:a-C films, and diffusion control in Ni:a-C films. It is known that foreign atoms or clusters migrate outward through encapsulated onion shells [10]. Therefore, it is presumed that the formation of spherical graphite shell structures around fine Fe grains make grain growth the interface reaction control because the permeability of the onion-like structures dominates the process. On the other hand, absence of graphitic layers around Ni grains in the interior of the film makes it the diffusion control.
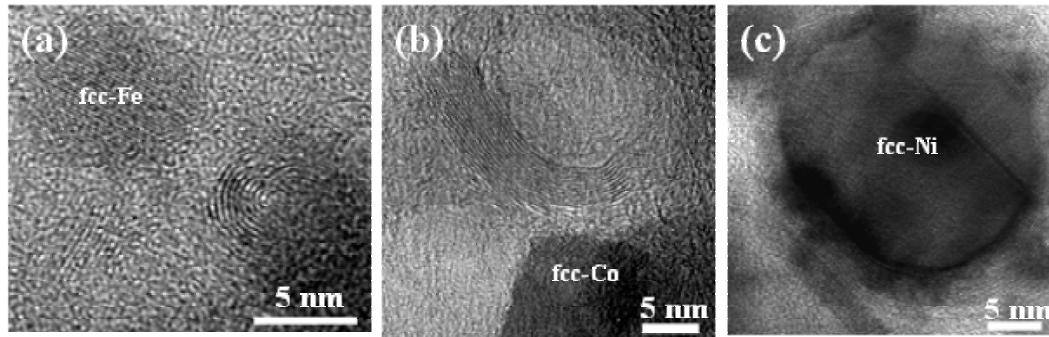
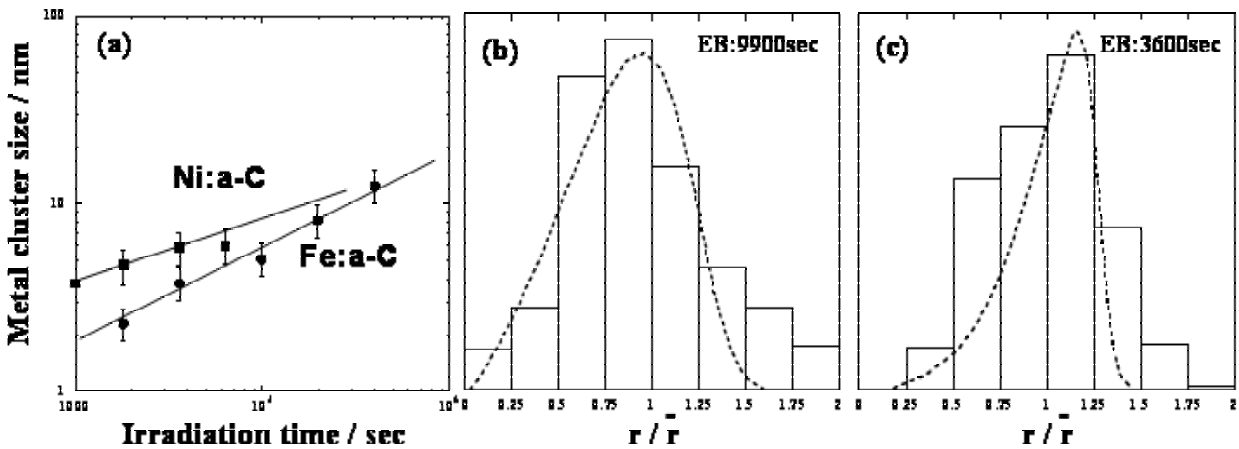Figure 5. Graphitic structures formed in Fe:a-C, Co:a-C and Ni:a-C films.

Figure 6. (a) Average metal grain size as a function of EB irradiation time. (b) Size distribution of Fe grains. (c) Size distribution of Ni grains.

The graphitization behavior in contact with Fe, Co and Ni observed in situ in TEM was precisely reported in the literature [10-11]. The formation of curved multi-shell structures observed in this study implied that the graphitization process is similar to that observed by Banhart in which spherical graphitic shells form at the interface of the metal grains following shrinkage of the encapsulated crystals. The plate-like graphitic structures were observed in Fe:a-C and Co:a-C. This graphitization seems to be independent to the metal grains. Since the plate-like structures formed in the area where carbon did not contact the metal grains anymore and the size was far larger than that of the metal grains, the formation mechanisms is believed to be different from that of the onion-like structures. It is presumed that the graphitization is significant rearrangement of carbon network in the film independent of metal grains.

Conclusions

Nano-composite structures containing graphitic clusters in an amorphous carbon matrix was synthesized by modifying metal containing amorphous carbon thin films using low-

energy electron beam irradiation. Two types of graphitization behavior were observed: spherical multi-shell structures which are strongly related to metal grains and relatively large plate-like structures which appear to be a significant rearrangement of amorphous carbon network in the film independent of metal grains. It is suggested that the carbon hybrid structures can be controlled by concentration or distribution of the metal elements. As this process is operated at a relatively low temperature and performed at a reduced or even atmospheric pressure, it can be easily applied to practical applications.

References

[1] Ugarte D. Curling and Closure of Graphitic Networks under Electron-beam Irradiation. Nature 1992;359:707-709.

[2] Sjostrom H, Stafstrom S, Boman M and Sundgren J-E. Superhard and Elastic Carbon Nitride Thin Films Having Fullerenelike Microstructure. Phys. Rev. Lett. 1995;75:1336-1339.

[3] Amaratunga GAJ, Chhowalla M, Kiely CJ, Alexandrou I, Ahrronov R, Devenish RM. Hard Elastic Carbon Thin Films from Linking of Carbon Nanoparticles. Nature 1996;383: 321-323.

[4] Chhowalla M, Ahrronov RA, Kiely CJ, Alexandrou I, Amaratunga GAJ. Generation and Deposition of Fullerene- and Nanotube-rich Carbon Thin Films. Philosophical Magazine Lett. 1997;75(5):329-335.

[5] Burden AP, Silva SRP. Fullerene-like Carbon nanoparticles Generated by Radio-frequency Plasma-enhanced Chemical Vapor Deposition. Philosophical Magazine Lett. 1998;78(1):15-19.

[6] Lavrentiev V, Abe H, Yamamoto S, Naramoto H, Narumi K. Formation of Carbon Nanotubes under Conditions of Co+C60 Film. Physica B 2002;323:303-305.

[7] Fujita J, Ishida M, Ichihashi T, Ochiai Y, Kaito T, Matsui S. Graphitization of Fe-doped Amorphous Carbon Pillers Grown by Focused-ion-beam-induced Chemical-vapor Deposition. J.Vac.Sci.Technol. 2002;B20:2686-2689.

[8] Lee CS, Kim TY, Lee KR, Ahn JP, Yoon KH. Nanocomposite ta-C Films Prepared by The Filtered Vacuum Arc Process Using Nanosized Ni Dots on a Si Substrate. Chem. Phys. Lett. 2003;380:774-779.

[9] Iwamura E. Structural Ordering of Metal-containing Amorphous Carbon Thin Films Induced by Low-energy Electron Beam Projection. Rev.Adv.Mater.Sci. 2003;5:34-40.

[10] Banhart F, Redlich P, Ajayan PM. The migration of Metal Atoms through Carbon Onions. Chem. Phys. Lett. 1998;292:554-560.

[11] Banhart F, Grobert N, Terrones M, Charlier JC, Ajayan PM. Metal Atoms in Carbon Nanotubes and Related Nanoparticles. International J. Modern Physics 2001;B15:4037-4069.